

Jet Quenching versus Jet Enhancement: a quantitative study of the BDMPS-Z gluon radiation spectrum

Urs Achim Wiedemann

Theory Division, CERN, CH-1211 Geneva 23, Switzerland

October 24, 2018

We study the gluon radiation spectrum off a hard in-medium produced quark in the multiple soft rescattering formalism of Baier-Dokshitzer-Mueller-Peigné-Schiff, and of Zakharov (BDMPS-Z). Its dependence on the quark and gluon energy, on the gluon transverse momentum, on the in-medium pathlength and on the rescattering properties of the nuclear medium is analyzed quantitatively. The two components of gluon radiation, the hard vacuum radiation associated to the quark production vertex, and the medium-induced rescattering contribution interfere destructively. For small spatial extensions of the medium, this destructive interference overcompensates the hard vacuum radiation, and the total medium-induced radiative energy loss decreases as $\Delta E \propto -L^3$. Medium-induced gluon production dominates only above a finite critical length $L > L_{\text{crit}}$ which varies between 3 and more than 6 fm depending on the rescattering properties of the medium. Deviations from the BDMPS- L^2 -behaviour persist above L_{crit} . The medium dependence of the angular gluon distribution is dominated by transverse Brownian \mathbf{k}_\perp -broadening. This results in a depletion of the low transverse momentum part of both the hard and the medium-induced contribution. As a consequence, the medium-induced energy loss outside a finite angular cone size Θ can be more than a factor two larger than the total medium-induced radiative energy loss. We discuss implications of these results for the jet quenching signal in relativistic heavy ion collisions at RHIC and LHC.

PACS numbers: 12.38.Bx; 12.38.Mh; 24.85.+p

Keywords: Radiative energy loss, QCD dipole cross section

1. Introduction

It is a longstanding goal to establish observables which characterize in a model-independent way the non-perturbative properties of a nuclear medium. The medium-dependence of perturbatively calculable “hard probes” is studied intensively to this end. A rigorous example available in e-A and p-A collisions is the generalized factorization theorem¹ of Luo, Qiu and Sterman (LQS) which relates the medium-dependence of a class of high- k_t observables to a very

small set of higher twist parton distribution functions of the cold target nucleus. For ultrarelativistic A-A collisions, we are not aware of a corresponding factorization theorem for observables which could be measured with existing or designed experiments at RHIC or LHC. This makes it interesting to search outside the framework of higher twist parton distributions for other, rather process-independent medium characterizations which allow to distinguish experimentally between the non-perturbative properties of hot and cold nuclear matter.

A good candidate for a one-parameter characterization of non-perturbative medium properties is the rescattering parameter $n_0 C$ obtained in the QCD dipole picture²⁻⁵. It describes the average squared transverse momentum transferred from the medium to an ultrarelativistic hard parton within one unit of pathlength, $n_0 C = \langle \mathbf{q}_\perp^2 \rangle / L$. This parameter increases with increasing nuclear density n_0 and (as a consequence of the equipartition theorem, $\langle \mathbf{q}_\perp^2 \rangle \propto T$) with increasing temperature. However, in order to characterize on the basis of $n_0 C$ differences between hot and cold nuclear matter, one has to understand quantitatively the sensitivity of different observables to $n_0 C$. To this end, we study here the dependence of the medium-induced one gluon radiation spectrum off a hard quark on the rescattering parameter $n_0 C$.

Medium-induced radiative energy loss and the associated phenomenon of “jet quenching” was proposed a decade ago by Gyulassy and Wang^{6,7} as a sensitive probe of the non-perturbative properties of excited nuclear matter. Baier, Dokshitzer, Mueller, Peigné and Schiff (BDMPS) established³ that its dominant contribution comes from the rescattering of the emitted gluon and results in a quadratic L^2 -increase of $\Delta E/E$. An equivalent^{8,5} path-integral formulation^{2,9} was derived independently by Zakharov (Z) - we refer to the formalism as BDMPS-Z. Recently, the present author⁵ derived the \mathbf{k}_\perp -differential extension (2.1) of this path-integral formalism which determines the transverse momentum distribution of the emitted gluon. Equation (2.1), the starting point of the present work, differs from other formulations^{10,11} by a regularization prescription^{4,5} which makes it applicable to finite size media. In particular, (2.1) shows in an opacity expansion⁵ the correct interpolation between totally coherent and totally incoherent radiation spectrum for spatially finite media. As we recall in section 3, the medium-dependence of (2.1) is determined by the rescattering parameter $n_0 C$ only.

Quantitatively, little is known about the one gluon radiation spectrum in the soft multiple scattering approximation. For the total, \mathbf{k}_\perp -integrated energy loss ΔE , numerical results by Zakharov¹² indicate weak deviations from the BDMPS- L^2 -law. However, a systematic study of its dependence on the rescattering parameter $n_0 C$ and the energy E of the incident quark is missing. Moreover, all existing results on ΔE are obtained by integrating the transverse gluon momentum up to infinity. In particular, it remains unclear to

what extent deviations from the BDMPS- L^2 -law become more significant if the finite kinematical boundary of the \mathbf{k}_\perp -integration and the proper regularization of the gluon radiation spectrum are taken into account. Also, there are no results which establish to what extent the main contribution to ΔE stems from the region of small gluon energy $\frac{\omega}{E} = x \ll 1$ and small transverse gluon momentum $|\mathbf{k}_\perp| \ll \omega$ to which the multiple soft rescattering formalism applies. This motivates a systematic study of the x - and \mathbf{k}_\perp -differential gluon radiation spectrum. The only related quantitative study due to Baier, Dokshitzer, Mueller and Schiff¹⁰ determines from the \mathbf{k}_\perp -differential radiation spectrum the phenomenologically important fraction $R(\Theta)$ of the energy ΔE radiated outside a cone of opening angle Θ . However, also in this study, the $|\mathbf{k}_\perp|$ -integration extends to infinity and the questions listed above remain to be answered. This is done in the present work which is organized as follows:

In section 2, we recall the main properties of the one-gluon radiation spectrum derived in the soft multiple scattering approximation. Section 3 collects analytical expressions obtained in the dipole approximation. Numerical results for the gluon radiation spectrum are presented in section 4 and their implications are discussed in the Conclusions.

2. The medium-induced radiation spectrum

We are studying the medium-induced, \mathbf{k}_\perp -differential one gluon radiation spectrum off a hard quark. In the multiple soft rescattering formalism, it reads⁵

$$\begin{aligned} \frac{d^3\sigma^{(*)}}{d(\ln x) d\mathbf{k}_\perp} &= \frac{\alpha_s}{(2\pi)^2} \frac{1}{\omega^2} N_C C_F 2\text{Re} \int_{z_-}^{z_+} dy_l \int_{y_l}^{z_+} d\bar{y}_l e^{-\epsilon|y_l| - \epsilon|\bar{y}_l|} \\ &\times \int d\mathbf{u} e^{-i\mathbf{k}_\perp \cdot \mathbf{u}} e^{-\frac{1}{2} \int_{\bar{y}_l}^{z_+} d\xi n(\xi) \sigma(\mathbf{u})} \frac{\partial}{\partial \mathbf{y}} \cdot \frac{\partial}{\partial \mathbf{u}} \mathcal{K}(\mathbf{y} = 0, y_l; \mathbf{u}, \bar{y}_l | \omega). \end{aligned} \quad (2.1)$$

Here, \mathcal{K} denotes the two-dimensional path-integral

$$\mathcal{K}(\mathbf{r}(y_l), y_l; \mathbf{r}(\bar{y}_l), \bar{y}_l | \omega) \int \mathcal{D}\mathbf{r} \exp \left[\int_{y_l}^{\bar{y}_l} d\xi \left(i \frac{\omega}{2} \dot{\mathbf{r}}^2 - \frac{1}{2} n(\xi) \sigma(\mathbf{r}) \right) \right]. \quad (2.2)$$

The medium-dependence of (2.1) stems from the factor $n(\xi) \sigma(\mathbf{r})$, where $n(\xi)$ determines the density of scattering centers in the medium. The dipole cross section

$$\sigma(\mathbf{r}) = 2 C_A \int \frac{d\mathbf{q}_\perp}{(2\pi)^2} |a_0(\mathbf{q}_\perp)|^2 \left(1 - e^{-i\mathbf{q}_\perp \cdot \mathbf{r}} \right) \quad (2.3)$$

contains configuration space information on the strength of a single elastic differential scattering cross section $\propto |a_0(\mathbf{q}_\perp)|^2$.

The spectrum (2.1) describes: i) Gluon radiation off a hard *nascent* quark ($* = nas$) produced during the collision inside the medium at $z_- = 0$. This is the medium-dependence of the QCD analogue of the radiation spectrum associated to β -decay. ii) Gluon radiation off an incoming quark ($z_- = -\infty$, $* = in$) contained in the wavefunction of the projectile. This is the medium-dependence of the Gunion-Bertsch radiation spectrum¹³.

In the configuration-space formulation (2.1), the quark radiates a gluon at longitudinal position y_L (\bar{y}_L) in the amplitude (complex conjugate amplitude). The ϵ -regularization of this cross section does not commute with the $z_\pm \rightarrow \pm\infty$ limit which removes the cut-off of the longitudinal integration. To do this analytically, we consider a medium of finite longitudinal extension positioned along the longitudinal axis between 0 and L ,⁴. We split the longitudinal integrals into six parts

$$\int_{z_-}^{z_+} \int_{y_l}^{z_+} = \int_{z_-}^0 \int_{y_L}^0 + \int_{z_-}^0 \int_0^L + \int_{z_-}^L \int_{y_L}^{z_+} + \int_0^L \int_{y_L}^L + \int_0^L \int_L^{z_+} + \int_L^{z_+} \int_{y_L}^{z_+}. \quad (2.4)$$

The six corresponding contributions to the cross section are labelled in an obvious way:

$$\frac{d^3\sigma^{(*)}}{d(\ln x) d\mathbf{k}_\perp} = \frac{\alpha_s}{\pi^2} N_c C_F \sum_{j=1}^6 I_j. \quad (2.5)$$

Explicit expressions for the I_j 's, in which the limits $z_\pm \rightarrow \pm\infty$, $\epsilon \rightarrow 0$ are taken, are listed in Appendix A, Eqs. (A.2)-(A.7). They are the starting point of the following discussion. We recall several technical points:

1. Region of validity of (2.1)

Eq. (2.1) is obtained by assuming small angle multiple scattering for both the projectile quark and the radiated gluon³. Its region of validity is limited to $x \ll 1$ and $|\mathbf{k}_\perp| \ll \omega$. For the calculation of the total radiative energy loss, integration over x and \mathbf{k}_\perp is required. As discussed below, the x -integration is not problematic since the integrand has its main support at small x . The \mathbf{k}_\perp -integration, however, has significant support in the infrared and the ultraviolet regime.

2. Infrared behaviour of (2.1)

For vanishing medium thickness, the gluon radiation (2.1) off a nascent quark is proportional to $\frac{1}{\mathbf{k}_\perp^2}$, and the \mathbf{k}_\perp -integration is logarithmically divergent in the infrared. To subleading order $O(x)$, an additional term $\exp[-i\bar{q}(y_L - \bar{y}_L)]$

appears in the integrand of (2.1), with $\bar{q} \propto m_q^2$ the quark mass^{2,22,4}. This term provides a natural infrared cut-off. In the following analysis, however, we shall not modify (2.1) by terms subleading in $O(x)$. We shall rather subtract from (2.1) the medium-independent hard radiation associated with the quark production in vacuum. The medium-dependent remainder turns out to be infrared finite. This allows us to give a numerical analysis of the medium-induced radiative energy loss without depending on an infrared cutoff parameter.

3. Ultraviolet behaviour of (2.1)

The \mathbf{k}_\perp -integration over (2.1) is ultraviolet divergent even if the medium-independent part is subtracted off. This is no fundamental problem, since the transverse momentum is kinematically bound by the total energy of the gluon, $|\mathbf{k}_\perp| \in [0, \omega]$. It indicates, however, that the total radiative energy loss calculated from (2.1) is sensitive to the high transverse momentum modes $|\mathbf{k}_\perp| = O(\omega)$ which lie outside the region of validity of its derivation. This is discussed in section 4 E.

3. Dipole approximation

Two approximation schemes are known for the spectrum (2.1): the opacity expansion and the dipole approximation. In the first, one expands the spectrum in powers of the density of scattering centers^{4,5,15,16}. This also gives access to the radiation off a small finite number of scattering centers. In the dipole approximation, one exploits that the integrand of (2.1) has its main support at small transverse distances $r = |\mathbf{r}|$. This allows to write the dipole cross section (2.3) to logarithmic accuracy as

$$\sigma(\mathbf{r}) = C r^2. \quad (3.1)$$

This approximation is used in all discussions of BDMPS^{3,8,10} and of Zakharov^{2,9,12,11}. It allows to explore the multiple soft rescattering regime in which Brownian motion dominates⁴. Due to (3.1), the path-integral in (2.1) simplifies to that of a harmonic oscillator

$$\mathcal{K}_{\text{osz}}(\mathbf{y}, y_t; \mathbf{u}, \bar{y}_t | \mu) = \frac{A}{\pi i} \exp \left[i A B (\mathbf{y}^2 + \mathbf{u}^2) - 2 i A \mathbf{y} \cdot \mathbf{u} \right], \quad (3.2)$$

$$A = \frac{\mu \Omega}{2 \sin(\Omega \Delta y)}, \quad B = \cos(\Omega \Delta y), \quad (3.3)$$

with complex oscillator frequency

$$\Omega = \frac{1-i}{\sqrt{2}} \sqrt{\frac{n_0 C}{\omega}}. \quad (3.4)$$

$$I_6 = \frac{1}{\mathbf{k}_\perp^2} . \quad (3.10)$$

The contribution I_6 is exactly (i.e. without taking recourse to the dipole approximation) the medium-independent contribution associated to the hard radiation off a nascent quark jet propagating in the vacuum⁵. This follows from the leading $O(x)$ approximation in which only the rescattering of the radiated gluon contributes. Subtracting the medium-independent term I_6 , the medium-induced modification to the hard radiation spectrum is given by I_4 and I_5 ,

$$\frac{d^3\sigma_{med}^{(nas)}}{d(\ln x) d\mathbf{k}_\perp} = \frac{\alpha_s}{\pi^2} N_c C_F (I_4 + I_5) . \quad (3.11)$$

The radiation spectrum (2.5) is positive, of course, since one cannot radiate less than no gluon. This positivity is guaranteed by the sum $I_4 + I_5 + I_6 > 0$ which according to (3.6) forms a complete square. For the difference (3.11) between the radiation spectrum (2.5) and the corresponding vacuum contribution, positivity is not warranted: if less gluons are emitted from the nascent off-shell quark in the medium than in the vacuum, then the medium-induced deviation turns negative. The interplay between negative (*jet enhancement*) and positive (*jet quenching*) values of (3.11) will be studied in what follows.

4. Numerical Results and Analytical Approximations

The \mathbf{k}_\perp -integration of (3.7)-(3.9) is infrared finite. Using polar coordinates

$$\bar{I}_j = \int_0^{2\pi} d\varphi_k \int_0^{\chi\omega} k_\perp dk_\perp I_j , \quad (4.1)$$

one finds

$$\begin{aligned} \bar{I}_4 = 4\pi \text{Re} \int_0^{\bar{L}} d\tilde{z}_1 \int_0^{\tilde{z}_1} d\tilde{z}_2 & \left(\frac{i}{2} \frac{1}{1 - \cosh[(1+i)\Delta\tilde{z}]} \right. \\ & \left. + \frac{i}{4} e^{-2M_c^2 \sinh[(1+i)\Delta\tilde{z}/2]/2} \frac{F}{N^2} \right) , \end{aligned} \quad (4.2)$$

$$\begin{aligned} F \equiv \tilde{z}_2^2 - 2i \coth[(1+i)\Delta\tilde{z}/2] & \left[(1+i)(M_c^2 + \tilde{z}_2) \right. \\ & \left. + \coth[(1+i)\Delta\tilde{z}/2] \right] , \end{aligned} \quad (4.3)$$

$$\bar{I}_5 = 4\pi \text{Re} \int_0^{\bar{L}} d\tilde{z} \left(\frac{-1}{2} \frac{1+i}{\sinh[(1+i)\tilde{z}]} \right)$$

$$+ \frac{(1+i) e^{-(1+i)M_c^2 \tanh[(1+i)\tilde{z}/2]}}{4 \sinh[(1+i)\tilde{z}/2] \cosh[(1+i)\tilde{z}/2]} \Big) . \quad (4.4)$$

Here, $\chi \in [0, 1]$ denotes the fraction of the maximal transverse momentum up to which we integrate, and M_c denotes the corresponding upper integration limit $\chi\omega$ in dimensionless rescaled variables

$$M_c = \frac{\chi\omega}{\sqrt{2\omega\sqrt{2}|\Omega|}} . \quad (4.5)$$

These expressions determine the x -differential radiation spectrum

$$\begin{aligned} \frac{d\sigma_{med}^{(nas)}}{d(\ln x)}(n_0 C, L, E, \chi) &= \int_{|\mathbf{k}_\perp| \leq \chi\omega} d\mathbf{k}_\perp \frac{d^3\sigma_{med}^{(nas)}}{d(\ln x) d\mathbf{k}_\perp} \\ &= \frac{\alpha_s}{\pi^2} N_c C_F \left(\bar{I}_4 + \bar{I}_5 \right) , \end{aligned} \quad (4.6)$$

which is a function of the rescattering parameter $n_0 C$, the pathlength L of the quark in the medium, the energy of the quark E and the kinematical cut-off χ . The χ -dependence of (4.6) allows to extract \mathbf{k}_\perp -differential information from the \mathbf{k}_\perp -integrated expression (4.6), see section 4 E below. The x -integrated total radiative energy loss ΔE is given by

$$\frac{\Delta E}{E}(n_0 C, L, E, \chi) = \int_0^1 dx x \frac{d\sigma_{med}^{(nas)}}{dx} . \quad (4.7)$$

A. Analytical Expansion for small L

1. Radiation off projectile quark

For the gluon radiation off an incoming quark, a Taylor expansion of the radiation spectrum (2.1) around $\tilde{L} = 0$ does not exist⁴. One finds

$$\begin{aligned} \frac{d^3\sigma^{(in)}}{d(\ln x) d\mathbf{k}_\perp} &= \frac{\alpha_s}{\pi^2} N_c C_F \left(\int \frac{d^2\mathbf{q}_\perp}{(2\pi)^2} \left(\frac{2\pi}{n_0 C L} \right) e^{-\frac{\mathbf{q}_\perp^2}{2n_0 C L}} \right. \\ &\times \left[\frac{1}{(\mathbf{q}_\perp - \mathbf{k}_\perp)^2} + 2 \frac{(\mathbf{q}_\perp - \mathbf{k}_\perp) \cdot \mathbf{k}_\perp}{(\mathbf{q}_\perp - \mathbf{k}_\perp)^2 \mathbf{k}_\perp^2} + \frac{1}{\mathbf{k}_\perp^2} \right] \Big) \left(1 + O(L^2) \right) + O(L^2) , \end{aligned} \quad (4.8)$$

which is non-analytic in L . The three contributions in the bracket $[]$ of (4.8) combine to

$$\propto \int \frac{d^2 \mathbf{q}_\perp}{(2\pi)^2} \left(\frac{2\pi}{n_0 C L} \right) e^{-\frac{\mathbf{q}_\perp^2}{2 n_0 C L}} \frac{\mathbf{q}_\perp^2}{(\mathbf{q}_\perp - \mathbf{k}_\perp)^2 \mathbf{k}_\perp^2}. \quad (4.9)$$

This is the Gunion-Bertsch gluon radiation spectrum¹³ for a target momentum transfer \mathbf{q}_\perp which is acquired by the transverse Brownian motion of the incoming projectile,

$$\langle \mathbf{q}_\perp^2 \rangle = 2 n_0 C L. \quad (4.10)$$

The dipole approximation does not break down for $L \rightarrow 0$ where the multiple soft rescattering formalism is questionable. Taking $L \rightarrow 0$ for $n_0 C L = \text{fixed}$, (4.9) matches smoothly onto the single Gunion-Bertsch rescattering result⁵.

2. Quark production in the medium

The medium-dependence (4.6) of the gluon radiation spectrum off a nascent quark can be expanded in a Taylor series for small in-medium pathlength. We find

$$\bar{I}_4 = \frac{1}{8} \tilde{L}^2 M_c^4 + \frac{1}{24} \tilde{L}^3 M_c^2 + O(\tilde{L}^4), \quad (4.11)$$

$$\bar{I}_5 = \frac{-1}{8} \tilde{L}^2 M_c^4 + \frac{-1}{12} \tilde{L}^3 M_c^2 + O(\tilde{L}^4). \quad (4.12)$$

Here, the destructive interference term \bar{I}_5 overcompensates for thin media the direct production term \bar{I}_4 . The resulting medium-induced deviation from the jet energy loss in the vacuum is negative,

$$\bar{I}_4 + \bar{I}_5 = \frac{-1}{24} \tilde{L}^3 M_c^2 + O(\tilde{L}^4). \quad (4.13)$$

The negative sign of this result indicates jet enhancement, i.e., the medium-dependence leads for small L to *harder* jet fragmentation functions. Shortly after the discovery of the EMC effect, Nachtmann and Pirner¹⁷ proposed a phenomenological picture which predicts harder fragmentation functions. To our knowledge, Eq. (4.13) is the first indication for such a jet enhancement effect in a QCD-motivated calculation. It will be discussed quantitatively in sections 4 B-4 E.

3. QCD dipole phenomenology

The rescattering parameter $n_0 C$ is the only model-dependent input of the medium-dependent gluon radiation spectrum (3.11). It characterizes the av-

erage squared transverse momentum transferred from the medium to the projectile per unit pathlength, see Eq. (4.10). We study this spectrum for four different values of $n_0 C$:

1. $n_0 C = 0.1 \text{ fm}^{-3} = (63 \text{ MeV})^2/\text{fm}$
2. $n_0 C = 0.5 \text{ fm}^{-3} = (141 \text{ MeV})^2/\text{fm}$
3. $n_0 C = 1.0 \text{ fm}^{-3} = (200 \text{ MeV})^2/\text{fm}$
4. $n_0 C = 2.0 \text{ fm}^{-3} = (280 \text{ MeV})^2/\text{fm}$

We chose these values after finding in exploratory calculations that they scan the region between negligible total energy loss ($\Delta E/E < 3\%$ for $n_0 C = 0.1 \text{ fm}^{-3}$) and very significant energy loss ($\Delta E/E > 20\%$ for $n_0 C = 2.0 \text{ fm}^{-3}$).

Baier, Dokshitzer, Mueller and Schiff¹⁰ described the rescattering properties of the medium by the transport coefficient \hat{q} which satisfies $\hat{q} = 2 n_0 C$. They estimate $n_0 C = 0.05 \text{ GeV}^3 = (500 \text{ MeV})^2/\text{fm}$ for hot matter at a temperature $T = 250 \text{ MeV}$. For cold nuclear matter, their estimate $n_0 C = 0.0025 \text{ GeV}^3 = (111 \text{ MeV})^2/\text{fm}$ is based on the relation between the rescattering parameter $n_0 C$ and the gluon distribution $x G(x)$. In comparison, the two lower values ($n_0 C = 0.1 \text{ fm}^{-3}$ and $n_0 C = 0.5 \text{ fm}^{-3}$) of our study scan a reasonable range of possible values for cold nuclear matter, and the larger values of $n_0 C$ may be associated to excited nuclear matter.

In principle, the parameter $n_0 C$ can be determined phenomenologically for cold nuclear matter from the medium-dependence of hard processes. One approach³ is to relate $n_0 C$ to the parameter λ_{LQS} which characterizes in the LQS-factorization approach¹ the amount of transverse momentum transferred to the hard parton. A first determination from the dijet imbalance resulted in $\lambda_{\text{LQS}}^2 = 0.05 - 0.1 \text{ GeV}^2$ corresponding to an extremely large value $n_0 C = 0.3 - 0.6 \text{ GeV}^2/\text{fm}^1$. More recent studies^{18,19} use the much smaller value $\lambda_{\text{LQS}}^2 = 0.01 \text{ GeV}^2$. This is still larger than the above estimate based on the gluon distribution. Significant experimental and theoretical uncertainties remain. Especially, the connection between $n_0 C$ and λ_{LQS} assumes a direct connection between multiple soft and single secondary (hard) rescattering³. As a consistency check, one should extract $n_0 C$ also from observables sensitive to the multiple soft rescattering, as e.g. DIS nuclear structure functions²⁰. There, however, existing parametrizations show a non-negligible dependence of the dipole strength C on Bjorken x_{bj} ²¹ or \sqrt{s} ¹⁴ and it becomes important to compare the extracted parameters in the corresponding kinematical regimes. The present work does not aim at a phenomenological evaluation of existing $e - A$ and $p - A$ data which takes the above considerations into account. It rather scans the parameter space in the region $0.1 \text{ fm}^{-3} < n_0 C < 2.0 \text{ fm}^{-3}$ which interpolates between cold and hot nuclear matter.

B. L -dependence of radiative energy loss

As long as not stated otherwise, we present the \mathbf{k}_\perp -integrated expressions (4.6), (4.7) for the kinematical boundary $\chi = 1$. All numerical results are for a strong coupling constant $\alpha_s = 1/3$ and $N_c = 3$.

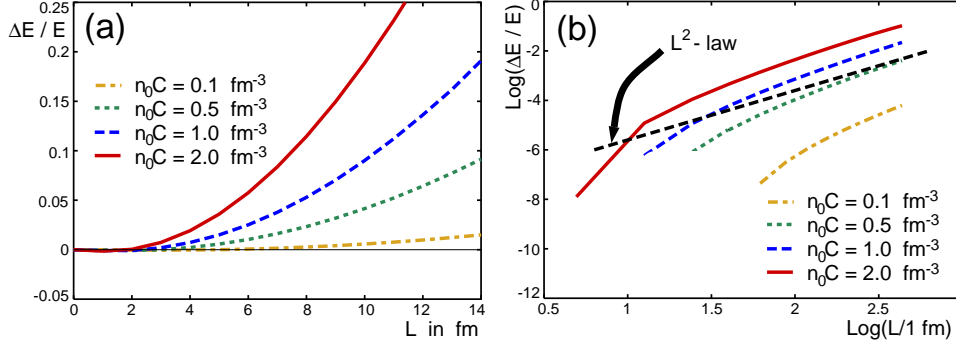


Fig. 1. (a) Dependence of the medium-induced radiative energy loss (4.7) on the in-medium pathlength L for $E = 100$ GeV, $\chi = 1$ and different values of the rescattering parameter $n_0 C$. (b) Double logarithmic presentation of (a) which indicates deviations from the BDMPS- L^2 -law.

Fig. 1(a) shows the L -dependence of the total radiative energy loss (4.7) off a hard quark of initial energy $E = 100$ GeV. Irrespective of the value of the rescattering parameter $n_0 C$, the total radiative energy loss $\Delta E/E$ increases stronger than linear. The double logarithmic plot Fig. 1(b) of the same calculation displays deviations from the BDMPS- L^2 -law³.

For sufficiently large L ($L < 14$ fm), the increase of the radiative energy loss is approximately $\propto L^{2.5}$. At smaller values of L ($L < 6$ fm), the radiation spectrum shows a numerically very small increase and turns negativ. This is consistent with the analytical result (4.13) and prevents us from extending the double logarithmic plot Fig. 1(b) into the small L region.

The sensitivity of the total radiative energy loss on the rescattering parameter $n_0 C$ depends strongly on the size of the in-medium pathlength. For $L > 8$ fm, a measurement of $\Delta E/E$ with an accuracy of $\approx 5\%$ would be sufficiently sensitive to distinguish between different values of the rescattering parameter $n_0 C$. For smaller in-medium pathlengths, however, this sensitivity is lost rapidly. To further analyze the region of negative $\Delta E/E$ and the delayed onset of significant total radiative energy loss, we turn now to the x -dependence of this spectrum.

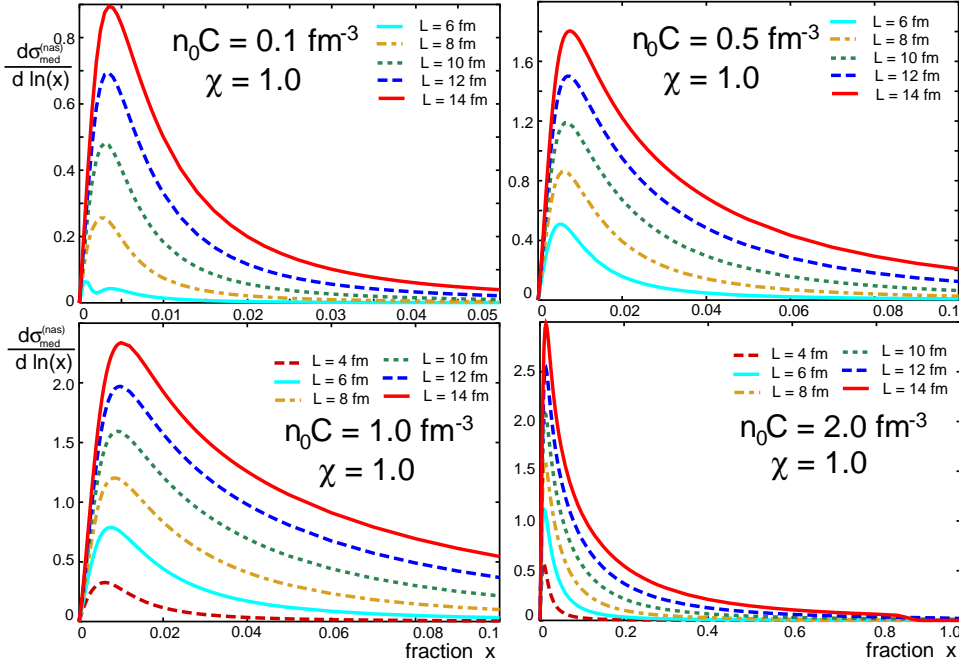


Fig. 2. The x -differential gluon radiation spectrum (4.6) as a function of x for different in-medium pathlengths L , and different values of the rescattering parameter $n_0 C$.

C. x -dependence of the gluon radiation spectrum

Fig. 2 shows for relatively large in-medium pathlengths L the x -differential radiation spectrum (4.6) which enters the calculation of the total medium-induced radiative energy loss (4.7). The spectrum peaks generically at very small values of x . This is an important consistency check since the derivation of the radiation spectrum (2.1) is based on the assumption $x \ll 1$.

The maximal radiation probabilities shown in Fig. 2 exceed unity for sufficiently large pathlength L . This may be taken as an indication that multiple gluon emission plays an important role for sufficiently extended targets.

In Fig. 3, the same x -differential radiation spectrum is plotted for relatively small in-medium pathlengths. The distinction between “large” and “small” is made empirically by the onset of more complicated structures in the radiation spectrum. The only purpose of presenting Fig. 3 separately from Fig. 2 is to make these structures better visible.

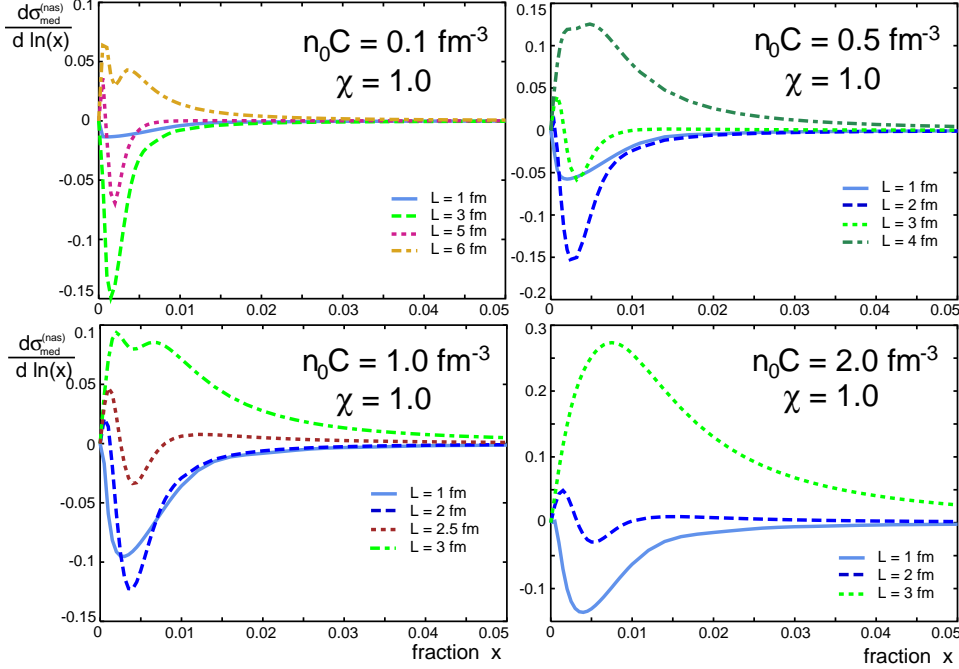


Fig. 3. The same as Fig. 2, but for relatively small pathlengths L of the quark in the medium. The destructive interference between hard and medium-induced radiation (“jet enhancement”) overcompensates the medium-induced gluon radiation (“jet quenching”) for sufficiently small L .

Irrespective of the value of the rescattering parameter $n_0 C$, the x -differential medium-induced gluon radiation spectrum Fig. 3 turns negative for very small pathlengths L . This is a consequence of the destructive interference between hard and medium-induced radiation. As one increases L , more medium-induced radiation amplitudes become available. Whether these lead to a stronger destructive interference with the hard radiation associated to the quark production vertex, or whether they lead to an increasing gluon emission probability depends on the quantitative interplay between in-medium pathlength L and the rescattering property $n_0 C$ of the medium. For $n_0 C = 0.1 \text{ fm}^{-3}$ in the upper right panel of Fig. 3, we observe e.g. that the destructive interference effect increases up to $L < 4 \text{ fm}$. Only for larger pathlengths, the medium-induced gluon production probability finally overcompensates the destructive interference term and the x -differential and x -integrated medium-induced energy loss turns positive.

According to Fig. 3, the pathlength at which exact compensation between medium-induced radiation and destructive interference occurs shows a strong $n_0 C$ -dependence. It decreases from $L \approx 5 \text{ fm}$ at $n_0 C = 0.1 \text{ fm}^{-3}$ via ($L \approx 3 \text{ fm}$, $n_0 C = 0.5 \text{ fm}^{-3}$) and ($L \approx 2.5 \text{ fm}$, $n_0 C = 1.0 \text{ fm}^{-3}$) up to ($L \approx 2.0 \text{ fm}$, $n_0 C = 2.0 \text{ fm}^{-3}$). This decrease with increasing $n_0 C$ is consistent with the picture that a significant transverse momentum transfer to the gluon is

needed to kick it out of the kinematical region in which destructive interference can occur.

Quantitatively, jet enhancement ($\Delta E < 0$) at small pathlengths is very small. It is almost invisible in the x -integrated radiation spectrum of Fig. 1. However, it delays the onset of a positive jet quenching contribution. As seen from Fig. 3, this offset depends significantly on the rescattering parameter $n_0 C$ of the medium. It will be further quantified in the next subsection.

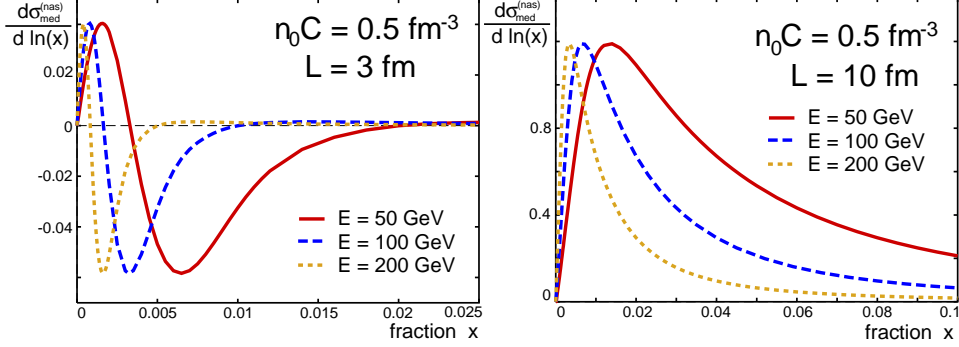


Fig. 4. The energy dependence of the x -differential radiation spectrum results in a simple x -scaling (4.14)

D. Energy dependence of the gluon radiation spectrum

In the gluon radiation spectrum (2.1), the energy E of the initial quark comes always multiplied by the fraction x of the energy carried away by the gluon. This implies a trivial x -scaling of the radiation spectrum as a function of energy,

$$\frac{d\sigma_{med}^{(nas)}}{d(\ln x)}(nC, L, E, x) = \frac{d\sigma_{med}^{(nas)}}{d(\ln x)}(nC, L, E', \frac{E}{E'}x). \quad (4.14)$$

In Fig. 4, we show illustrative examples of this scaling behaviour for a small pathlength (where destructive interference effects are important) and for a large pathlength.

If the x -differential radiation spectrum vanishes sufficiently fast at large x , the x -scaling (4.14) results (as a function of $1/E$) in a linear increase of the area under the x -differential radiation spectrum. Then, the total radiative energy loss $\left[\frac{\Delta E}{E}\right]$ scales as a function of energy like

$$\left[\frac{\Delta E}{E}\right](E) = \frac{E'}{E} \left[\frac{\Delta E}{E}\right](E'). \quad (4.15)$$

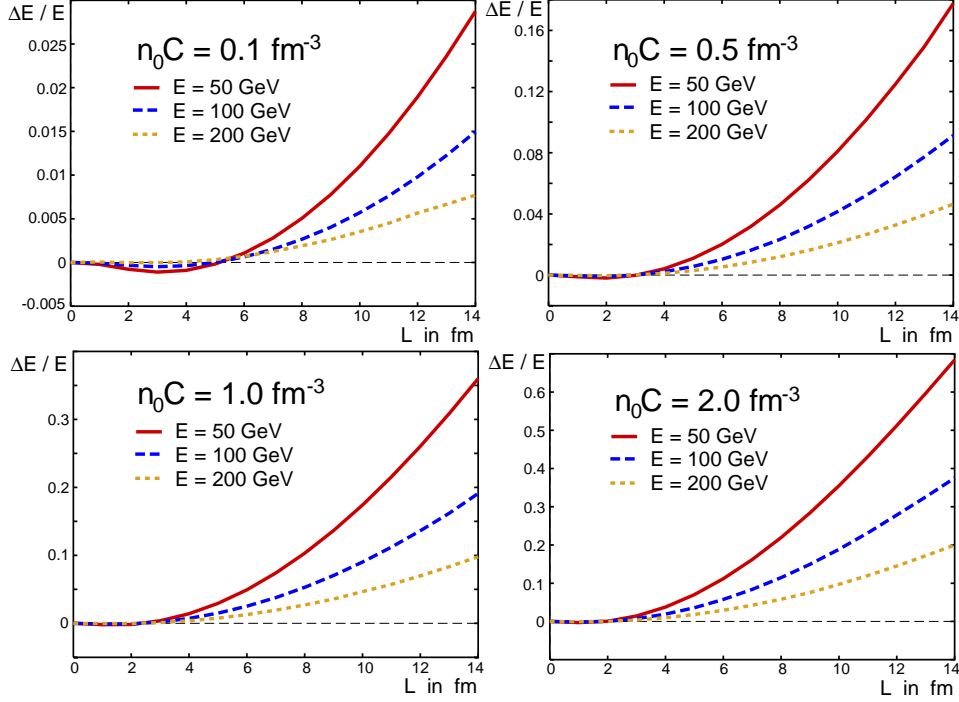


Fig. 5. L -dependence of the fraction of medium-induced total radiative energy loss (4.7) for different values of the initial parton energy E and different values of the rescattering parameter $n_0 C$ of the nuclear medium.

As can be seen from Fig. 5, the value of $\Delta E/E$ doubles approximately if one scales the initial parton energy by a factor $\frac{1}{2}$. This is consistent with the scaling law (4.15). It holds to good accuracy for all values of the rescattering parameter $n_0 C$ and for all physically realistic pathlengths L :

Fig. 5 also illustrates a property of the radiation spectrum consistent with factorization: One expects on general grounds that for increasing incident quark energy and fixed spatial extension of the medium, the medium-induced changes to the parton fragmentation become negligible in the limit $E \rightarrow \infty$. This is the naive factorization limit in which high momentum spectra depend on the initial parton distributions only, and do not test properties of the medium. Fig. 5 shows a significant decrease of the medium-induced fraction of radiative energy loss $\Delta E/E$ with increasing jet energy E . However, it indicates a kinematical sweetspot where initial parton energies are sufficiently high ($E > 50 - 100$ GeV) to make jet quenching a perturbatively calculable quantity and yet sufficiently small ($E < 1$ TeV say) so that the dependence on $n_0 C$ is still significant and makes jet quenching a sensitive probe of non-perturbative medium properties.

Another way of looking at Fig. 5 is by plotting the corresponding critical length L_{crit} above which the total radiative energy loss is larger than one percent,

$$\Delta E/E(L_{\text{crit}}) \equiv 0.01. \quad (4.16)$$

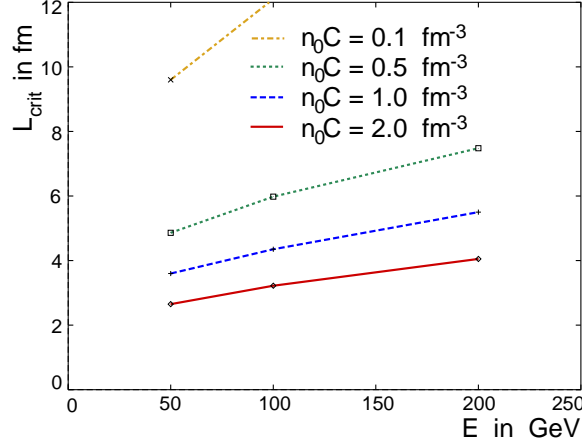


Fig. 6. The critical in-medium pathlength L_{crit} above which the medium-induced gluon radiation off the quark exceeds one percent of the total quark energy

As seen in Fig. 6, L_{crit} increases slowly with the incident energy of the parton. This is a consequence of the factorization limit: for a medium of finite extension, there is an initial parton energy above which medium-induced deviations of the parton fragmentation function become negligible. Also, L_{crit} increases obviously if the medium transfers less transverse momentum to the rescattering parton. L_{crit} ranges typically between 3 fm and more than 6 fm. This is a consequence of the interplay between jet enhancement at small L and jet quenching at large L which shifts the onset of a significant radiative energy loss to larger values of the in-medium pathlength L . Taking the finite geometry of ultrarelativistic heavy ion collisions into account²³, this effect may lead to a significant reduction of the jet quenching signal at RHIC and LHC since L_{crit} is of the same order as the in-medium pathlength of a substantial fraction of the produced jets.

E. Angular contribution to the radiative energy loss radiation spectrum

The χ -dependence of the radiation spectrum (4.6) allows to calculate the gluon radiation within an angular segment $\Delta \mathbf{k}_{\perp} \in [|\mathbf{k}_{\perp 1}|, |\mathbf{k}_{\perp 2}|]$, specified by $\chi_1 = (|\mathbf{k}_{\perp 1}|/\omega)$ and $\chi_2 = (|\mathbf{k}_{\perp 2}|/\omega)$,

$$\frac{d\sigma_{\text{med}}^{(\text{nas})}}{d(\ln x)}(nC, L, E, \Delta \mathbf{k}_{\perp}) =$$

$$\frac{d\sigma_{med}^{(nas)}}{d(\ln x)}(nC, L, E, \chi_2) - \frac{d\sigma_{med}^{(nas)}}{d(\ln x)}(nC, L, E, \chi_1). \quad (4.17)$$

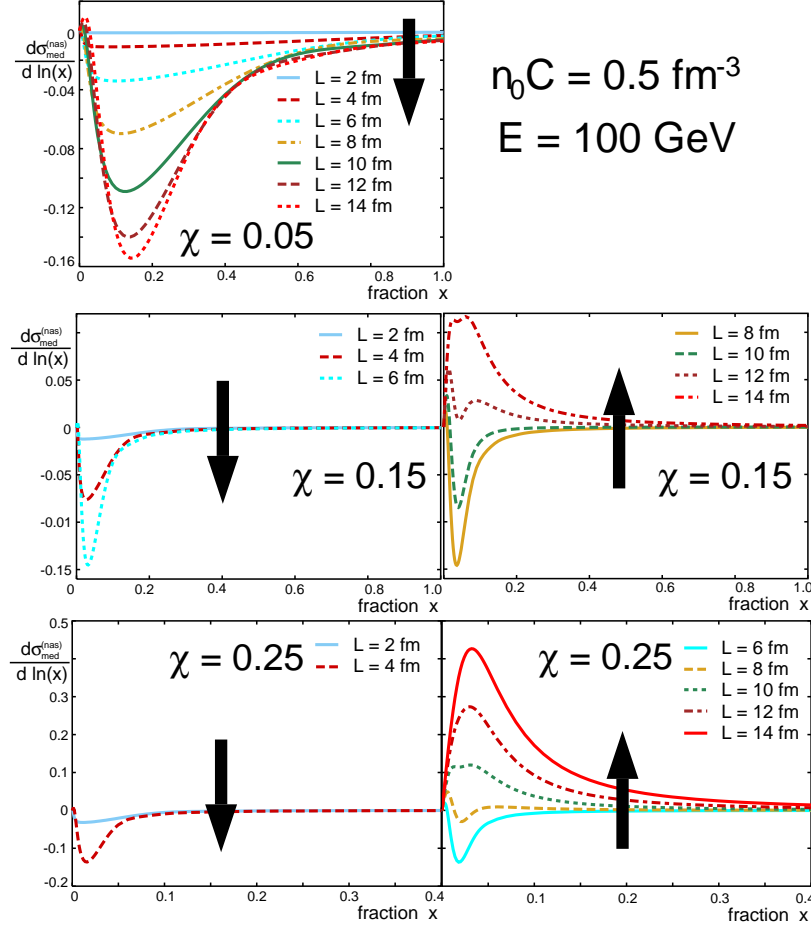


Fig. 7. The contributions to the \mathbf{k}_\perp -integrated radiation spectrum, coming from the phase space region $|\mathbf{k}_\perp| \in [0, \chi\omega]$ for $\chi = 0.05, 0.15$ and 0.25 . Arrows indicate how the spectrum changes with increasing in-medium pathlength L .

In Fig. 7, this spectrum is shown for $\chi_1 = 0$ and small values of $\chi_2 = \chi \ll 1$. For very small transverse momenta $|\mathbf{k}_\perp| < 0.05\omega$, we find that the radiation spectrum is significantly depleted over the whole range of available gluon energies $x \in [0, 1]$. This depletion continues to increase with increasing path length L even for rather large L , $L = 14$ fm. Increasing the upper bound on the transverse momentum $|\mathbf{k}_\perp| < \chi\omega$ to $\chi = 0.15$ and $\chi = 0.25$, one observes that the depletion turns into an enhancement for sufficiently large pathlength.

Even for large x ($x > 0.5$), a significant depletion of the spectrum occurs at small transverse momenta ($\chi = 0.05$) but disappears if higher transverse momenta are included ($\chi = 0.15$). This cannot be the result of destructive

interference since it does not show up in the \mathbf{k}_\perp -integrated radiation spectrum. It comes from the shifting of the gluon transverse phase space distribution which can be understood in terms of a classical multiple soft rescattering. In a classical picture, one expects a characteristic broadening of the hard radiation (3.11),

$$\frac{1}{\mathbf{k}_\perp^2} \longrightarrow \frac{1}{(\mathbf{k}_\perp + \mathbf{q}_\perp)^2} \quad (4.18)$$

as a function of the \mathbf{q}_\perp -momentum transfer which grows by Brownian motion $\langle \mathbf{q}_\perp^2 \rangle \propto L$. This leads to a depletion of the low \mathbf{k}_\perp momentum region of the radiation spectrum without affecting the \mathbf{k}_\perp -integrated spectrum. In contrast, the destructive interference between hard and medium-induced radiation discussed in section 4 C and also present in Fig. 7 affects the \mathbf{k}_\perp -integrated spectrum.

Comparing the absolute values of the radiation spectrum for $\chi = 0.05, 0.1$ and 0.15 shown in Fig. 7 with the absolute values of the $\chi = 1$ radiation spectrum in Figs. 2 and 3, one finds that the main contribution to the radiative energy loss (4.7) comes from gluons emitted at relatively large transverse momenta $|\mathbf{k}_\perp| > 0.25\omega$. However, the derivation of the gluon radiation spectrum (2.1) assumes $|\mathbf{k}_\perp| \ll \omega^{3,9,5}$. We conclude that the calculation of the BDMPS-Z total radiative energy loss receives its main contribution from a kinematical region in which the validity of the BDMPS-Z approximation is not guaranteed. This is not a feature of the dipole approximation studied here: numerical results of Gyulassy, Levai and Vitev¹⁶ indicate that also in the opacity expansion the dominant contribution to the radiative energy loss is obtained from gluons with significant transverse momentum.

F. Radiative energy loss outside a finite jet cone

From the χ -dependence of the x -integrated radiative energy loss (4.7), we can calculate the quantity

$$\frac{\Delta E}{E}(\Theta = \arcsin(\bar{\chi})) = \frac{\Delta E}{E}(\chi = 1) - \frac{\Delta E}{E}(\bar{\chi}). \quad (4.19)$$

This describes the fraction of the medium-induced relative radiative energy loss $\frac{\Delta E}{E}$ radiated outside a cone of opening angle Θ . Our notation in (4.19) suppresses the dependence of $\frac{\Delta E}{E}(\Theta)$ on the rescattering parameter $n_0 C$, the in-medium pathlength L , the quark energy E and the fraction x of the energy taken away by the gluon. Numerical results for (4.19) are shown in Fig. 8 for relatively large in-medium pathlengths and in Fig. 9 for the small pathlengths

for which the destructive interference between hard and medium-induced gluon production is significant.

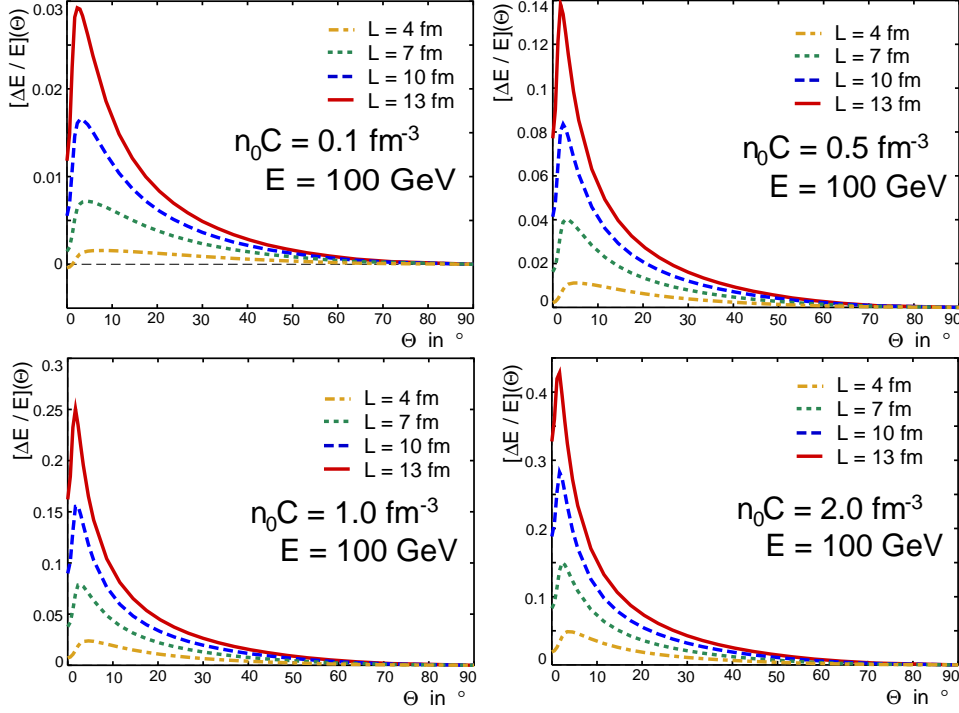


Fig. 8. The fraction (4.19) of the total radiative energy loss $\Delta E/E$ emitted outside a jet cone of fixed angle Θ .

As seen from Fig. 8, $\frac{\Delta E}{E}(\Theta)$ does not decrease monotonously with increasing Θ but has a maximum at finite jet opening angle. The reason is that the radiative energy loss outside a cone angle Θ receives additional contributions from the Brownian \mathbf{k}_\perp -broadening (4.18) of the hard vacuum radiation term I_6 . Such contributions do not affect the total \mathbf{k}_\perp -integrated yield $\frac{\Delta E}{E}(\Theta = 0)$, since they result only in a shifting of the transverse momentum phase space distribution of the emitted gluon. However, this shift in transverse phase space shows up as soon as a finite cone size is chosen. We conclude from Fig. 8 that the total \mathbf{k}_\perp -integrated radiative energy loss $\frac{\Delta E}{E}(\Theta = 0)$ is not the upper bound for the radiative energy loss outside a finite jet cone angle $\frac{\Delta E}{E}(\Theta)$. Depending on the rescattering parameter $n_0 C$ and the in-medium pathlength, the latter can be larger by more than a factor 2.

Fig. 9 displays the angular dependence (4.19) for a small in-medium pathlength where destructive interference becomes important. For the total \mathbf{k}_\perp -integrated radiative energy loss $\frac{\Delta E}{E}(\Theta = 0)$, the figure shows the small negative values discussed above and consistent with the analytical result (4.13). Outside a small opening angle $\Theta \approx 5^\circ$, however, the medium-induced radiative energy loss turns positive. This is again the effect of Brownian \mathbf{k}_\perp -broadening

which populates the high transverse momentum region.

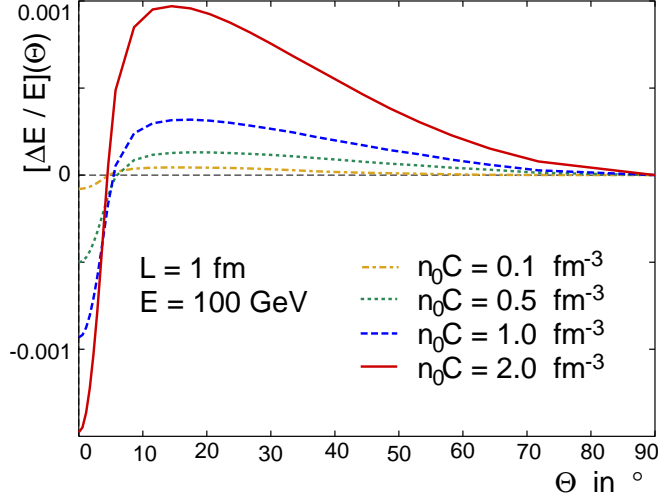


Fig. 9. Same as Fig. 8, but for small in-medium pathlength $L = 1$ fm.

5. Conclusion

In the above analysis of the medium-induced one-gluon radiation spectrum (3.11), we found that the hard radiation component associated to the in vacuum production of a hard quark is affected by i) medium-induced radiation and ii) medium-induced rescattering. Both effects are non-negligible in a quantitative analysis.

The first phenomenon is the destructive interference between hard (vacuum) and medium-induced radiation. For small in-medium pathlength, analytical and numerical results indicate that the hard parton radiates less energy in the medium than in the vacuum. This jet enhancement effect is numerically small. At larger pathlength, it is overcompensated by a positive medium-induced radiative energy loss. However, a quantitatively important remainder of jet enhancement is the delayed onset of significant jet quenching. In comparison to an unmodified L^2 -law, the hard parton has to propagate through a medium of larger spatial extension $L > L_{\text{crit}}$ in order to lose a detectable fraction of its total energy. In relativistic heavy ion collisions, the finite geometry limits the maximal extension of the in-medium pathlength. The values of L_{crit} between 3 and 6 fermi found in our analysis, may thus imply a significant reduction of the observed jet quenching signal.

The second phenomenon is the Brownian \mathbf{k}_\perp -broadening of the hard radiation due to multiple scattering. This shifts the \mathbf{k}_\perp -distribution of the hard (vacuum) component to higher transverse momenta. Subtracting the vacuum

contribution, one finds that the fraction of the total radiative energy loss $R(\Theta)$ in (4.19) emitted outside a jet angle Θ can be more than a factor 2 larger than the total medium-induced radiative energy loss obtained for $\Theta = 0^\circ$. In contrast to naive expectation, the total \mathbf{k}_\perp -integrated medium-induced radiative energy loss is not an upper bound on the medium-induced radiation outside a finite cone. In relativistic heavy ion collisions, this rescattering effect may imply a significant enhancement of the jet quenching signal.

Quantitative statements about the gluon radiation spectrum depend on the energy E of the projectile parton, the in-medium pathlength L and the rescattering parameter $n_0 C$ which is the only model-parameter in our discussion. For the spectrum (3.11), we have studied these dependencies in detail. The suggested analysis strategy for experimental data is to determine $n_0 C$ for normal cold nuclear matter phenomenologically and then to compare to the values extracted in relativistic heavy ion collisions. The rescattering parameter can be related in model calculations to the non-perturbative rescattering properties of the hot or cold nuclear medium. In this sense, $n_0 C$ is a model parameter which can be extracted from experimental data and which allows to distinguish between different physical pictures of the excited nuclear medium.

The present work is restricted to the analysis of the one-gluon radiation spectrum (3.11) derived in the BDMPS-Z formalism. It was one purpose of our quantitative study to clarify the kinematical region of validity of this approach. In particular, we found that the small- x gluon emission probabilities are very high. This indicates the importance of multiple gluon radiation which is not contained in the BDMPS-Z formalism. Moreover, the BDMPS-Z formalism is based on the assumption of small transverse gluon momentum $|\mathbf{k}_\perp| \ll \omega$ while we find the main contribution to radiative energy loss for $|\mathbf{k}_\perp| = O(\omega)$. Both features question the validity of the BDMPS-Z formalism and await further work. We emphasize, however, that the physical origin of the two qualitatively novel effects discussed here, appears to be very generic. Even outside the BDMPS-Z formalism, we expect that the destructive interference between hard and medium-induced radiation, and the strong implications of Brownian \mathbf{k}_\perp -broadening for radiation outside a finite jet cone, leave similar, quantitatively important traces in the medium-induced gluon radiation spectrum.

A. Simplifying the radiation spectrum (3.11)

This appendix contains details of how to turn the radiation cross section (2.1) into a numerically accessible form. We consider a nuclear medium of homogeneous density affecting the propagation of the hard quark in the longitudinal interval $[0, L]$. Replacing the in-medium propagator $\mathcal{K}(\mathbf{y}, y_l; \mathbf{u}, \bar{y}_l | \omega)$ outside $[0, L]$ by the free propagator \mathcal{K}_0 ,

$$\mathcal{K}_0(\mathbf{y}, y_l; \mathbf{u}, \bar{y}_l | \omega) = \frac{\omega}{2\pi i(\bar{y}_l - y_l)} \exp\left(\frac{i\omega(\mathbf{y} - \mathbf{u})^2}{2(\bar{y}_l - y_l)}\right), \quad (\text{A.1})$$

the ϵ -regularization in (2.1) can be removed analytically⁴. Replacing the constraint $\mathbf{y} = 0$ in (2.1) by a representation of the δ -function, $\int d\mathbf{y} \frac{d\mathbf{p}_\perp}{(2\pi)^2} \exp(-i\mathbf{p}_\perp \cdot \mathbf{y})$, one finds

$$I_1 = \text{Re} \int \frac{d^2\mathbf{p}_\perp}{(2\pi)^2} \int d\mathbf{u} e^{-i\mathbf{u} \cdot (\mathbf{k}_\perp + \mathbf{p}_\perp)} e^{-\frac{1}{2}n_0 \sigma(\mathbf{u})} \frac{1}{\mathbf{p}_\perp^2} \quad (\text{A.2})$$

$$I_2 = \frac{\text{Re}}{\omega} \int_0^L d\bar{y}_L \int \frac{d^2\mathbf{p}_\perp}{(2\pi)^2} \int d\mathbf{u} d\mathbf{r} e^{-i\mathbf{p}_\perp \cdot \mathbf{r} - i\mathbf{k}_\perp \cdot \mathbf{u}} \times e^{-\frac{1}{2}(L - \bar{y}_L)n_0 \sigma(\mathbf{u})} \frac{\mathbf{p}_\perp}{\mathbf{p}_\perp^2} \cdot \frac{\partial}{\partial \mathbf{u}} \mathcal{K}(\mathbf{r}, 0; \mathbf{u}, \bar{y}_l | \omega), \quad (\text{A.3})$$

$$I_3 = 2\text{Re} \int \frac{d^2\mathbf{p}_\perp}{(2\pi)^2} \frac{\mathbf{p}_\perp \cdot \mathbf{k}_\perp}{\mathbf{p}_\perp^2 \mathbf{k}_\perp^2} \int d\mathbf{r}_1 d\mathbf{r}_2 e^{-i\mathbf{p}_\perp \cdot \mathbf{r}_1 - i\mathbf{k}_\perp \cdot \mathbf{r}_2} \mathcal{K}(\mathbf{r}_1, 0; \mathbf{r}_2, L | \omega), \quad (\text{A.4})$$

$$I_4 = \frac{2\text{Re}}{4\omega^2} \int_0^L dy_L \int_{y_L}^L d\bar{y}_L \int d\mathbf{u} e^{-\frac{1}{2}(L - \bar{y}_L)n_0 \sigma(\mathbf{u})} \times e^{-i\mathbf{k}_\perp \cdot \mathbf{u}} \frac{\partial}{\partial \mathbf{y}} \cdot \frac{\partial}{\partial \mathbf{u}} \mathcal{K}(\mathbf{y} = 0, y_l; \mathbf{u}, \bar{y}_l | \omega), \quad (\text{A.5})$$

$$I_5 = \frac{\text{Re}}{2\omega} \int_0^L dy_L \int d\mathbf{u} e^{-i\mathbf{k}_\perp \cdot \mathbf{u}} \frac{\mathbf{k}_\perp}{\mathbf{k}_\perp^2} \cdot \frac{\partial}{\partial \mathbf{y}} \mathcal{K}(\mathbf{y} = 0, y_L; \mathbf{u}, L | \omega), \quad (\text{A.6})$$

$$I_6 = \frac{1}{\mathbf{k}_\perp^2}. \quad (\text{A.7})$$

In the dipole approximation, these expressions take the form

$$I_1 = \int \frac{d^2\mathbf{p}_\perp}{(2\pi)^2} \frac{1}{\mathbf{p}_\perp^2} \left(\frac{2\pi}{n_0 C L} \right) \exp\left[-\frac{(\mathbf{k}_\perp + \mathbf{p}_\perp)^2}{2n_0 C L}\right] \quad (\text{A.8})$$

$$I_2 = \frac{\text{Re}}{\omega} \int_0^L dy_L \left(\frac{A(1 - B^2)}{DB + iA(1 - B^2)} \exp\left[-\frac{B\mathbf{k}_\perp^2}{4[DB + iA(1 - B^2)]}\right] \times \left(-1 + \exp\left[\frac{\mathbf{k}_\perp^2}{4[DB + iA(1 - B^2)]} \frac{A}{AB + iD}\right] \right) + \frac{A}{DB + iA(1 - B^2)} \frac{-iD}{AB + iD} \exp\left[-\frac{\mathbf{k}_\perp^2}{4(D - iAB)}\right] \right) \quad (\text{A.9})$$

$$I_3 = \text{Re} \frac{2\pi}{iA(1 - B^2)} \int \frac{d\mathbf{p}_\perp}{(2\pi)^2} \frac{\mathbf{p}_\perp \cdot \mathbf{k}_\perp}{\mathbf{p}_\perp^2 \mathbf{k}_\perp^2} \times \exp\left[\frac{i(B\mathbf{p}_\perp^2 + 2\mathbf{p}_\perp \cdot \mathbf{k}_\perp + B\mathbf{k}_\perp^2)}{4A(1 - B^2)}\right], \quad (\text{A.10})$$

$$I_4 = \frac{1}{4\omega^2} 2\text{Re} \int_0^L dy_l \int_{y_l}^L d\bar{y}_l \left(\frac{-4A^2 D}{(D - iAB)^2} + \frac{iA^3 B \mathbf{k}_\perp^2}{(D - iAB)^3} \right)$$

$$\times \exp \left[-\frac{\mathbf{k}_\perp^2}{4(D - i A B)} \right], \quad (\text{A.11})$$

$$I_5 = \frac{1}{\omega} \text{Re} \int_0^L dz \frac{-i}{B_z^2} \exp \left[-i \frac{\mathbf{k}_\perp^2}{4 A_z B_z} \right], \quad (\text{A.12})$$

$$I_6 = \frac{1}{\mathbf{k}_\perp^2}. \quad (\text{A.13})$$

The variables A , B and D introduced here have different arguments for the different terms:

$$A_2 = A_5 = \frac{\omega \Omega}{2 \sin(\Omega y_L)}, \quad B_2 = B_5 = \cos(\Omega y_L), \quad (\text{A.14})$$

$$A_3 = \frac{\omega \Omega}{2 \sin(\Omega L)}, \quad B_3 = \cos(\Omega L), \quad (\text{A.15})$$

$$A_4 = \frac{\omega \Omega}{2 \sin(\Omega(\bar{y}_L - y_L))}, \quad B_4 = \cos(\Omega(\bar{y}_L - y_L)), \quad (\text{A.16})$$

$$D_2 = \frac{1}{2} n_0 C(L - y_L), \quad D_4 = \frac{1}{2} n_0 C(L - \bar{y}_L). \quad (\text{A.17})$$

-
1. M. Luo, J.W. Qiu, and G. Sterman, Phys. Rev. **D49** (1994) 4493; ibidem **D50** (1994) 1951.
 2. B.G. Zakharov, JETP Letters **63** (1996) 952; ibidem **65** (1997) 615.
 3. R. Baier, Y.L. Dokshitzer, A.H. Mueller, S. Peigné and D. Schiff, Nucl. Phys. **B483** (1997) 291; ibidem **B484** (1997) 265.
 4. U.A. Wiedemann and M. Gyulassy, Nucl. Phys. **B560** (1999) 345.
 5. U.A. Wiedemann, hep-ph/0005129, Nucl. Phys. **B** in press.
 6. X.-N. Wang and M. Gyulassy, Phys. Rev. **D44** (1991) 3501.
 7. M. Gyulassy and X.-N. Wang, Nucl. Phys. **B420** (1994) 583.
 8. R. Baier, Y.L. Dokshitzer, A.H. Mueller and D. Schiff, Nucl. Phys. **B531** (1998) 403.
 9. B.G. Zakharov, Phys. Atom. Nucl. **61** (1998) 838 [Yad. Fiz. **61** (1998) 924], hep-ph/9807540.
 10. R. Baier, Y.L. Dokshitzer, A.H. Mueller and D. Schiff, Phys. Rev. **C60** (1999) 064902.
 11. B.G. Zakharov, JETP Lett. **70** (1999) 176.
 12. B.G. Zakharov, talk given at 33rd Recontres de Moriond, Les Arcs, France, March 21-28, 1998; hep-ph/9807396.
 13. J.F. Gunion and G. Bertsch, Phys. Rev. **D 25** (1982) 746.
 14. B.Z. Kopeliovich, A. Schäfer and A.V. Tarasov, Phys. Rev. **D62** (2000) 054022.
 15. M. Gyulassy, P. Levai and I. Vitev, Nucl. Phys. **B571** (2000) 197.

- 16. M. Gyulassy, P. Levai and I. Vitev, nucl-th/0005032 and nucl-th/0006010.
- 17. O. Nachtmann and H.J. Pirner, Ann. Physik Leipzig 44 (1987) 13.
- 18. X.F. Guo, Phys. Rev. **D58** (1998) 114033.
- 19. R.J. Fries, A. Schäfer, E. Stein and B. Müller, Phys. Rev. Lett. **83** (1999) 4261 and Nucl. Phys. **B582** (2000) 537.
- 20. U.A. Wiedemann, Nucl. Phys. **B582** (2000) 409.
- 21. K. Golec-Biernat and M. Wüsthoff, Phys. Rev. **D59** (1999) 014017; ibidem **D60** (1999) 074012.
- 22. B.Z. Kopeliovich, A. Schäfer and A.V. Tarasov, Phys. Rev. **C59** (1999) 1609.
- 23. I.P. Lokhtin and A.M. Snigirev, Phys. Lett. **B440** (1998) 163. and hep-ph/0004176.